

Comparison of ^{87}Rb N -resonances for D_1 and D_2 transitions

Irina Novikova, David F. Phillips, Alexander S. Zibrov*, Ronald L. Walsworth¹ and Alexksei V. Taichenachev, Valeriy I. Yudin²

¹Harvard-Smithsonian Center for Astrophysics and Department of Physics, Harvard University, Cambridge, MA, 02138, USA

²Institute of Laser Physics SB RAS and Novosibirsk State University, Novosibirsk, 630090, Russia
(Dated: September 18, 2018)

We report an experimental comparison of three-photon-absorption resonances (known as “ N -resonances”) for the D_1 and D_2 optical transitions of thermal ^{87}Rb vapor. We find that the D_2 N -resonance has better contrast, a broader linewidth, and a more symmetric lineshape than the D_1 N -resonance. Taken together, these factors imply superior performance for frequency standards operating on alkali D_2 N -resonances, in contrast to coherent population trapping (CPT) resonances for which the D_2 transition provides poorer frequency standard performance than the D_1 transition.

PACS numbers:

Recently, we demonstrated that three-photon-absorption resonances known as “ N -resonances” [6, 7, 8] are a promising alternative to coherent population trapping (CPT) resonances [1, 2, 3, 4, 5] for small atomic frequency standards using thermal alkali vapor. In this letter, we report an experimental comparison of N -resonances for the ^{87}Rb D_1 ($5^2\text{S}_{1/2} \rightarrow 5^2\text{P}_{1/2}$, $\lambda = 795$ nm) and D_2 ($5^2\text{S}_{1/2} \rightarrow 5^2\text{P}_{3/2}$, $\lambda = 780$ nm) optical transitions. We find similar N -resonance quality factors for the D_1 and D_2 transitions, but a significantly more symmetric lineshape for the D_2 transition, which together implies superior performance for a frequency standard using the D_2 N -resonance. Previous work has shown that the quality factor of alkali CPT resonances is about an order of magnitude worse for D_2 operation than for D_1 . [9, 10] Thus, as current miniature frequency standards rely on vertical-cavity surface emitting lasers (VCSELs) that are readily available for the D_2 transitions of Rb and Cs but more difficult to acquire for the D_1 transitions, the results reported here provide an additional practical advantage for the N -resonance.

An N -resonance is a three-photon, two-optical-field absorptive resonance (Fig. 1a). A probe field, Ω_P , resonant with the transition between the higher-energy hyperfine level of the ground electronic state and an electronically excited state, optically pumps the atoms into the lower hyperfine level, leading to increased transmission of the probe field through the medium. A drive field, Ω_D is detuned from the probe field by the atomic hyperfine frequency, ν_0 . Together, Ω_P and Ω_D create a two-photon Raman resonance that drives atoms coherently from the lower to the upper hyperfine level, thereby inducing increased absorption of the probe field Ω_P in a narrow resonance with linewidth, $\Delta\nu$, set by ground-state hyperfine decoherence. Attractive features of N -resonances for atomic frequency standards include high resonance contrast, leading-order light-shift cancellation, and less sensitivity than CPT resonances to high buffer gases. [7, 8]

Better performance for N -resonances than CPT resonances on the D_2 transition is expected due to the dif-

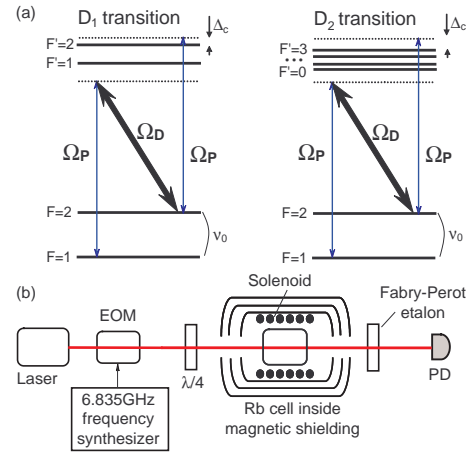


FIG. 1: (a) N -resonance interaction scheme for D_1 and D_2 transitions of ^{87}Rb . Ω_P and Ω_D are probe and drive optical fields that create and interrogate the N -resonance; ν_0 is the splitting of the ground-state hyperfine levels $F = 1$ and $F = 2$; and Δ_c is the one-photon detuning of the probe field from resonance between the $F = 2$ ground state and the excited state. (b) Schematic of the experimental setup. See text for abbreviations.

ference between the resonance mechanisms. The CPT transmission maximum appears as a result of optical pumping of atoms into a non-interacting coherent superposition of two ground-state hyperfine levels (a “dark state”). However, a pure dark state exists only for the D_1 transition, thus the amplitude and contrast of CPT resonances are much higher for D_1 operation than for D_2 . [9] For N -resonances, the three-photon absorptive process does not require a dark state, with no resultant advantage of D_1 over D_2 . Furthermore, for circularly polarized light (commonly used in optically-pumped atomic clocks) resonant with the D_1 transition, some atoms become trapped in the Zeeman state with maximum angular momentum — an “end” state ($F = 2, m_F = \pm 2$ for ^{87}Rb) — which limits resonance amplitude and contrast on the ground-state $\Delta m_F = 0$ hyperfine clock transition. However, for

D_2 operation, the end state is coupled to the excited state through the cycling transition $F = 2 \rightarrow F' = 3$. In the presence of strong collisional mixing in the excited state (induced by alkali-buffer gas collisions), the cycling transition suppresses optical pumping of atoms into the end state. Thus we expect higher resonance contrast for N -resonances operating on the D_2 transition.

Figure 1b shows a schematic of our N -resonance apparatus. We operated the system under conditions identified in our previous work to give good frequency standard performance.[7, 8] We derived the two optical fields Ω_P and Ω_D by phase modulating the output of an external cavity diode laser tuned to either the D_1 or D_2 transition of ^{87}Rb . Laser phase-modulation was performed at the ^{87}Rb ground-state hyperfine frequency ($\nu_0 \simeq 6.8$ GHz) by an electro-optic modulator (EOM) driven by an amplified microwave synthesizer phase-locked to a hydrogen maser. We used the +1 sideband as the probe field and the zeroth order carrier as the drive field. We set the laser detuning Δ_c and EOM modulation index to match the conditions for leading-order light-shift cancellation: [8] for D_1 , $\Delta_c \approx +700$ MHz from the $F = 2 \rightarrow F' = 2$ transition; for D_2 , $\Delta_c \approx +500$ MHz from the $F = 2 \rightarrow F' = 3$ transition; in both cases the modulation index ≈ 0.38 , corresponding to a probe/drive intensity ratio of about 19%. The laser beam was circularly polarized by a quarter wave plate ($\lambda/4$) and weakly focused to a diameter of 0.8 mm before entering a Pyrex cell of length 7 cm and diameter 2.5 cm containing isotopically enriched ^{87}Rb and 100 Torr of Ne buffer gas (which induced excited-state collisional broadening ≈ 2 GHz). We heated the cell to $\approx 65^\circ\text{C}$, yielding ^{87}Rb density $\approx 4 \cdot 10^{11}\text{cm}^{-3}$. We isolated the Rb vapor cell from external magnetic fields using three layers of high-permeability shielding, and applied a small (≈ 10 mG) longitudinal magnetic field to lift the degeneracy of the Zeeman sublevels and separate the $F = 1, m_F = 0$ to $F = 2, m_F = 0$ clock transition (with first order magnetic field independence) from the $m_F = \pm 1$ transitions with first order magnetic field sensitivity. The transmitted probe field power was detected by a photodetector (PD); the strong drive field and the off-resonant lower sideband were filtered from the transmitted laser beam by a quartz narrow-band Fabry-Perot etalon (FSR = 20 GHz, finesse = 30) tuned to the frequency of the probe field.

Figure 2 shows examples of measured D_1 and D_2 N -resonances under identical conditions, with the probe field transmission normalized to unity away from two-photon resonance. Figure 3 shows the measured dependence on laser intensity of the N -resonance contrast, linewidth, and quality factor. We define resonance contrast as $C = 1 - T_{min}/T_o$, where T_{min} and T_o are the transmitted probe field intensities on two-photon resonance and away from resonance, respectively. The linewidth, $\Delta\nu$, is the measured full-width-half-maximum (FWHM); and the resonance quality factor is $q = C/\Delta\nu$. [The shot-noise limit to atomic clock frequency stability is inversely proportional to the quality factor; i.e., larger

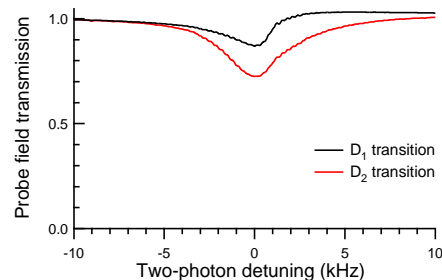


FIG. 2: Example ^{87}Rb N -resonances observed for D_1 and D_2 optical transitions. Laser power is $260 \mu\text{W}$, corresponding to an intensity of $50 \text{ mW}/\text{cm}^2$. Probe transmission is normalized to unity away from two-photon resonance.

q corresponds to better frequency stability. [1]) As seen in Figures 2 and 3, the typical measured N -resonance contrast is significantly larger for D_2 operation than for the D_1 transition, whereas the linewidth is broader for D_2 than for D_1 . The differences in contrast and linewidth largely offset each other, such that the N -resonance quality factor is roughly comparable for the D_1 and D_2 transitions over a wide range of operating conditions. Note that in alkali vapor CPT resonances, the quality factor for the D_2 transition has been measured to be about an order of magnitude smaller than for the D_1 transition.[9, 10]

Optically-probed atomic frequency standards commonly employ slow modulation of the microwave drive and associated phase-sensitive detection as part of the crystal oscillator lock-loop. Hence an asymmetric atomic resonance lineshape can induce systematic frequency shifts proportional to the modulation parameters.[11] As seen in Fig. 2, ^{87}Rb N -resonances are significantly more symmetric for the D_2 transition than for D_1 , which gives an important advantage for D_2 N -resonance operation. The relative asymmetry of the D_1 and D_2 N -resonance lineshapes can be quantified by describing each measured N -resonance as a combination of symmetric and antisymmetric Lorentzian functions:

$$T = T_o - \frac{A \Delta\nu/2 + B \delta}{\Delta\nu^2/4 + \delta^2} \quad (1)$$

where T is the measured probe field transmission as a function of two-photon Raman detuning, δ ; and A , B , and $\Delta\nu$ are fit parameters that represent the amplitudes of the symmetric and antisymmetric Lorentzian components and the resonance linewidth. Fig. 4 shows the ratio of antisymmetric and symmetric components, B/A , determined from our N -resonance lineshape measurements, as a function of laser intensity, indicating that the D_1 N -resonance is typically more than an order of magnitude more asymmetric than the D_2 N -resonance.

In conclusion, N -resonances are three-photon-absorption resonances that are a promising alternative to CPT resonances for small atomic frequency standards using alkali atoms. Here, we report an experimental comparison of the D_1 and D_2 N -resonances in thermal

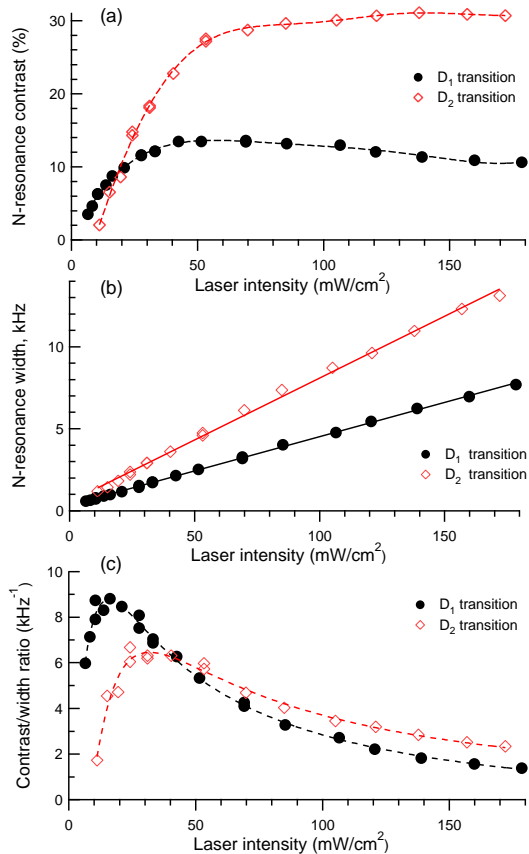


FIG. 3: N -resonance (a) contrast C , (b) linewidth $\Delta\nu$, and (c) quality factor $q = C/\Delta\nu$, as a function of total input laser intensity, measured on the ^{87}Rb D_1 (solid circles) and D_2 (open diamonds) transitions. Dashed lines are to guide the eye.

^{87}Rb vapor. We find that the D_2 N -resonance has better contrast but a broader linewidth than the D_1 N -resonance, such that the N -resonance quality factor is comparable for the D_1 and D_2 transitions. This

result implies a similar shot-noise-limit to N -resonance frequency standard performance on the D_1 and D_2 transitions — in stark contrast with CPT resonances for which the quality factor is about an order of magnitude worse for the D_2 transition than for D_1 . In addition, we find that the D_2 N -resonance lineshape is significantly more symmetric than the D_1 lineshape, indicating that a D_2 N -resonance frequency standard will have reduced sensitivity to certain modulation-induced systematic frequency shifts. Thus, unlike for CPT resonances, commercially available diode lasers for the D_2 lines of Rb and Cs can likely be used without compromising the performance of an N -resonance frequency standard.

The authors are grateful to J. Vanier and M. Cresci-manno for useful discussions. This work was supported by ONR, DARPA, ITAMP and the Smithsonian Institution. A. V. T. and V. I. Y. acknowledge support from RFBR (grants no. 05-02-17086, 05-08-01389 and 04-02-

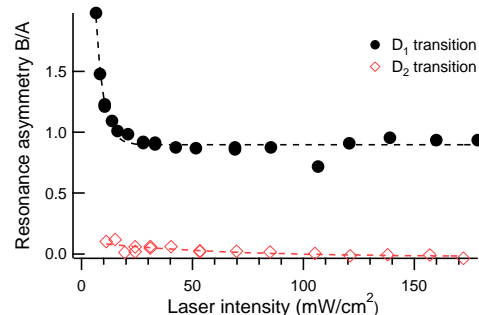


FIG. 4: N -resonance asymmetry, B/A , as a function of laser intensity, determined from fits of a combination of symmetric and antisymmetric Lorentzian functions to measured N -resonance lineshapes; for D_1 (solid circles) and D_2 (open diamonds) transitions. Dashed lines are to guide the eye.

16488). I. Novikova's e-mail address: i.novikova@osa.org.
 * also at Lebedev Institute of Physics, Moscow, Russia.

-
- [1] J. Vanier, *Appl. Phys. B* **81**, 421 (2005).
 [2] S. Knappe, P. D. D. Schwindt, V. Shah, L. Hollberg, J. Kitching, L. Liew, and J. Moreland, *Opt. Express* **13**, 1249 (2005).
 [3] P. D. D. Schwindt, S. Knappe, V. Shah, L. Hollberg, J. Kitching, L. Liew, and J. Moreland, *Appl. Phys. Lett.* **85**, 6409 (2004).
 [4] A. B. Matsko, D. Strekalov, and L. Maleki, *Opt. Commun.* **247**, 141 (2005).
 [5] M. Merimaa, T. Lindwall, I. Tittonen, and E. Ikonen, *J. Opt. Soc. Am. B* **20**, 273 (2003).
 [6] A. S. Zibrov, C. Y. Ye, Y. V. Rostovtsev, A. B. Matsko, and M. O. Scully, *Phys. Rev. A* **65**, 043817 (2002).
 [7] S. Zibrov, I. Novikova, D. F. Phillips, A. V. Taichenachev, V. I. Yudin, R. L. Walsworth, and A. S. Zibrov, *Phys. Rev. A* **72**, 011801(R) (2005).
 [8] I. Novikova, D. F. Phillips, A. S. Zibrov, R. L. Walsworth, A. V. Taichenachev, and V. I. Yudin, to appear in *Opt. Lett.* (2006).
 [9] M. Stahler, R. Wynands, S. Knappe, J. Kitching, L. Hollberg, A. Taichenachev, and V. Yudin, *Opt. Lett.* **27**, 1472, (2002).
 [10] R. Lutwak, D. Emmons, T. English, W. Riley, A. Duwel, M. Varghese, D. K. Serkland, and G. M. Peake, in *Proceedings of the 35th Annual Precise Time and Time Interval (PTTI) Systems and Applications Meeting*, U.S. Naval Observatory, Washington, D.C., 2003, p. 467.
 [11] D. F. Phillips, I. Novikova, C. Y.-T. Wang, M. Cresci-manno, and R. L. Walsworth, *J. Opt. Soc. Am. B* **22**, 305 (2005).